



Protonation of caffeine: A theoretical and experimental study



Hamed Bahrami, Mahmoud Tabrizchi*, Hossein Farrokhpour

Department of Chemistry, Isfahan University of Technology, Isfahan 84156-83111, Iran

ARTICLE INFO

Article history:

Received 21 September 2012

In final form 16 January 2013

Available online 26 January 2013

Keywords:

Caffeine

Proton Affinity

Ion Mobility

ABSTRACT

Protonation of caffeine was examined by ion mobility spectrometry equipped with two ionization sources, corona discharge (CD) and UV photoionization. Three peaks were observed in ion mobility spectrum by simultaneously running the two ionization sources. Experimental and theoretical evidence was collected to link the observed peaks to caffeine related ionic species. One peak was attributed to the M^+ ion while the other two were assigned to different protonated isomers of caffeine. In the case of CD ionization source, it was observed that different sites of caffeine compete for protonation and their relative intensities, depends on the sample concentration as well as the nature of the reactant ions. The new concept of “internal proton affinity” (IPA) was defined to express the tendency of holding the added proton for each atom in a molecule.

© 2013 Elsevier B.V. All rights reserved.

1. Introduction

The detection and measurement of caffeine (CAF) or trimethylxanthine ($M = 194$), as a central nervous system and metabolic stimulant [1], have attracted the attention of many researchers. Chromatography and mass spectrometry with different ionization sources have been widely used in the study of caffeine. Electrospray ionization mass spectrometric analysis of caffeine showed only one major peak at m/z 195, corresponding to non-fragmented protonated caffeine, MH^+ [2–4]. Atmospheric pressure photoionization (APPI), using a dopant, also exhibited only one major peak for caffeine at m/z 195 [5]. In addition, mass spectrum of caffeine with a nickel-63 ionization source showed two peaks for caffeine, corresponding to M^+ and MH^+ [6], while with corona discharge ionization source, only one peak at m/z 195 was shown [7]. Furthermore, determination of caffeine by means of LC–MS/MS with electrospray ionization in human plasma [8] and breast milk [9] showed only the protonated form of caffeine as non-fragmented product ion.

In addition to the above techniques, ion mobility spectrometry (IMS) has been used to measure caffeine in dietary supplement [10] and chewing gum [11]. Ion mobility spectrum of caffeine with electrospray ionization source showed only one product ion peak [12,13]. Distributed plasma ionization source (DPIS) for ion mobility spectrometry also led to one product ion peak for caffeine [14]. An old IMS–MS study of caffeine with radioactive ionization source at room temperature reviled four peaks, mainly nitrogen clusters of MH^+ and M_2^+ and an unknown ion at $m/z = 252$ [15].

Proton affinity (PA) is one of the most important thermodynamic quantities that link the thermochemistry of ions to that of the neutral molecules. The importance of proton transfer reactions in chemistry and biochemistry made the researchers to be increasingly involved in theoretical calculation and experimental measurement of proton affinities and gas phase basicities (GB). There are several experimental techniques, based on either chemical equilibrium or kinetic measurements, for determining the relative proton affinities. The techniques, including high-pressure mass spectrometry [16,17], fast atom bombardment mass spectrometry [18,19], Fourier-transform mass spectrometry [20], selected ion flow tube [21,22] and ion mobility spectrometry [23], can be used for proton affinity determination.

In the case of multifunctional molecules, such as caffeine (Fig. 1), there may be several sites for protonation. Experimental methods explore only the most stable protonated structures corresponding to the most basic sites in the molecule such that the topical proton affinities of less basic sites are missing in the experimental studies. Therefore, most experimental measurements of proton affinities should basically be supported by theoretical calculations [24–28]. The effect of molecular structure on proton affinity has been investigated in several papers [27,29,30]. For example, Wolken and Turecek [31] reported 25 theoretical proton affinities for uracil tautomers. The proton affinity of uracil obtained from the *ab initio* calculations for the most basic site was in good agreement with that derived from experimental measurements.

Here, we report a joint theoretical and experimental investigation of proton affinities of CAF as a test compound. In this study, we used an ion mobility spectrometer (IMS) for experimental measurements. The advantage of IMS is that unlike mass spectrometer, different protonated molecules with similar masses may be

* Corresponding author. Tel.: +98 311 3913272; fax: +98 311 3912350.

E-mail address: m-tabriz@cc.iut.ac.ir (M. Tabrizchi).

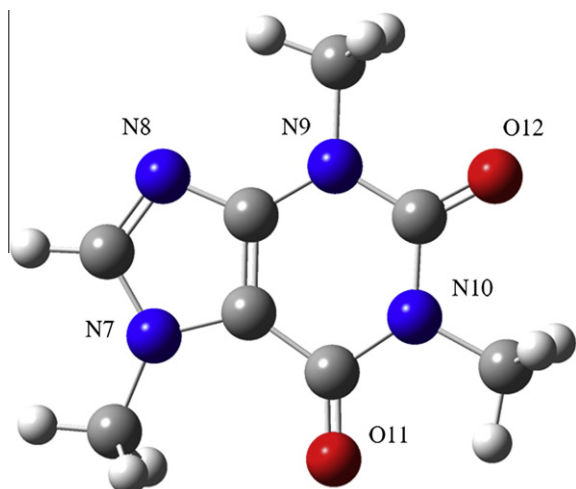


Fig. 1. Molecular structure of caffeine.

separated in IMS [32,33] because the size and the shape of the ion is also important in IMS.

All mass spectrometric studies at elevated temperatures, using corona discharge or electrospray ionization sources, revealed that the m/z 195, corresponding to MH^+ ion, appears in mass spectra. However, we observed two distinct peaks in ion mobility spectrum of CAF. The main objective of this work is to assign these two peaks to different isomers of MH^+ with the aid of calculated gas-phase thermochemical properties of CAF ion and its protonated cations. Additional experimental observations, obtained by using UV source and ion molecule reactions, are used to support the assignment and confirm the theoretical calculations.

2. Experimental

2.1. Instrument

All experiments were performed with an ion mobility spectrometer, constructed in our laboratory at Isfahan University of Technology [34]. To summarize, a continuous current of ions is pulsed by a shutter grid. The ion packet drifts under a constant electric field at atmospheric pressure. Ions are then separated in the drift region, based on their mobility, which depends on their mass, charge and size. The IMS instrument used in this study was equipped with two ionization sources: corona discharge (CD) and UV photoionization. The details of the UV ionization source and the geometry of the two sources as well as the experimental method have been given in Refs. [35,36]. For photoionization, a UV lamp was mounted parallel to the axis of the ion mobility cell. The corona discharge electrode was mounted perpendicular to the UV radiation. The design allows one to observe peaks from either the corona discharge or photoionization both individually and simultaneously. Thus, it is possible to compare accurately the peaks in the ion mobility spectra of each individual source.

The optimized experimental conditions are given in Table 1.

2.2. Sample preparation

Caffeine was purchased from Merck and used without further purification. Standard solutions of caffeine in water were prepared and working solutions in the range of 5–200 ppm were prepared by consecutive dilution. 2 μ L of the working solution was loaded into the injection port and the solvent was allowed to evaporate. Analytical grade toluene in vapor form was used as the dopant in

Table 1
The optimized experimental conditions.

Parameter	Setting
Length of drift tube	11 (cm)
Drift field	466 (V/cm)
Flow rate of drift gas (N_2)	800 (mL/min)
Flow rate of carrier gas (N_2)	300 (mL/min)
Flow rate of dopant (toluene)	300 (μ L/min)
Injection port temperature	220 ($^{\circ}$ C)
IMS cell temperature	200 ($^{\circ}$ C)
Polarity	Positive

the case of UV photoionization. Ammonia, in gas phase, was prepared through head space released from solid ammonium carbonate. A syringe pump (New Era Pump System Inc. USA) was used to inject headspace vapor of toluene or ammonia into the ionization region at a flow rate of 300 and 400 μ L/min, respectively.

2.3. Computational details

The theoretical calculations have been carried out with the quantum computational GAUSSIAN 09 package [37]. All of the calculations have been performed at two different levels of theory including Hartree–Fock (HF) and density functional theory (DFT). The geometry of the neutral, cation and different protonated CAF isomers was optimized at B3LYP, CAM-B3LYP and wB97X levels of theory using 6-311++G** basis set separately. The frequency calculations were performed on the optimized structures to search for the negative frequency and obtain the thermodynamic values such as enthalpy, Gibbs free and internal energy of the considered species. In addition, the volumes of the ions were calculated using the structures optimized at HF/aug-cc-pvdz and B3LYP/6-311++G** levels of theory.

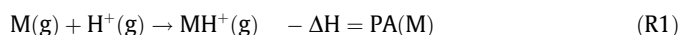
3. Results and discussion

3.1. Thermodynamic stability of isomers and proton affinity

Fig. 1 shows the molecular structure of CAF. As can be seen, there are several sites including the oxygen of carbonyl groups and the nitrogen of imine group (N8) for protonation.

To find the most stable protonated isomer of CAF, the neutral molecule was protonated from different sites (all nitrogen and oxygen). The geometry of the protonated isomers was optimized to select the most stable structures. The results of the geometry optimization for the most three stable isomers, relative electronic and Gibbs free energy, are reported in Table 2. The structure, protonated from the N8 site, $MH^+(N8)$, is the most stable one among the ions. The next stable isomers, $MH^+(O11)$ and $MH^+(O12)$, are about 5 kcal/mol less stable than the N8 protonated CAF. It should be noticed that the difference in the stability of the two oxygen protonated isomers is small, which is related to similar chemical environment around the oxygen atoms in the two isomers. The optimized structures of the protonated isomers reported in Table 2 were used for further theoretical studies.

The proton affinity (PA) of a molecule M is the negative of the enthalpy change of the protonation reaction:



The calculated enthalpies of the components contributing in reaction R1 were used to obtain the PA of CAF. Frequency calculations were performed on each component at 473 K, the temperature at which the ion mobility spectra were recorded. The enthalpy of proton at 473 K (2.331 kcal/mol) was taken from Ref. [38]. Table 3 reports the PA of the CAF when it is protonated from

Table 2

Relative electronic and Gibbs free energies at 473 K (in kcal/mol) of protonated caffeine isomers at different levels of theory.

Reference compound	B3LYP/6-311++G**		CAM-B3LYP/6-311++G**		wB97X/6-311++G**	
	E_{ele}	G	E_{ele}	G	E_{ele}	G
MH ⁺ (N8)	0	0	0	0	0	0
MH ⁺ (O11)	5.0586	3.9665	5.6438	4.5620	6.0519	3.8855
MH ⁺ (O12)	5.9718	4.9573	6.1587	5.0960	6.3061	4.9040

Table 3

The absolute proton affinities of caffeine for the three most favored protonation sites as well as water and ammonia at 473 K (in kcal/mol) using different levels of theory.

Compound	B3LYP/6-311++G**	CAM-B3LYP/6-311++G**	wB97X6-311++G**
MH ⁺ (N8)	218.728	217.011	219.374
MH ⁺ (O11)	213.061	210.788	212.762
MH ⁺ (O12)	212.087	210.190	212.459
H ₂ O	165.033	164.294	166.446
NH ₃	204.658	203.569	206.196

three different sites (N8, O11 and O12) at different levels of theory. Again, the protonation is more in favor of the N8 site. All proton affinities of CAF, given in Table 3, are higher than that of water; hence, the three forms of CAF.H⁺ may be formed in IMS when the reactant ion is H₃O⁺.

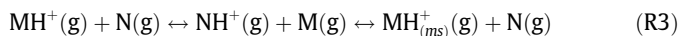
3.2. Internal proton affinity

For multifunctional compounds, there may be several possibilities for protonation. Among these, one protonated site is the most stable one and there is a possibility for converting the different protonated isomers to each other. Here, we define the “Internal Proton Affinity” (IPA) for MH⁺ as the enthalpy change of the following hypothetical reaction.



where MH_(ms)⁺ is the most stable form of the protonated molecule. The internal proton affinity is a measure of the desire for proton attraction among the different sites of the molecule. It reflects the internal competition for holding the proton. Unlike PA, which is defined for molecules, the IPA is only defined for protonated ions. The IPA for the MH_(ms)⁺ is zero and since it is a relative quantity, its values are negative for the rest of isomer ions. The calculated values of IPA's for different forms of protonated CAF are given in Table 4.

In Reaction 2, the protonated ion is rearranged and the reaction may be called an “internal proton transfer reaction”. The reaction, i.e., transferring proton, may happen quantum mechanically. In this reaction, the rate depends on the activation energy as well as the distance between the two sites involved in the exchange [39]. The reaction may also take place through a third body, capable of exchanging proton.



This different from the third body collision in the formal sense. Here the third body means a species that takes the proton from one body and donates to a second body. In fact, it acts as a species that catalyzes the reaction.

3.3. Ion mobility spectra

Tracing *a* and *b*, Fig. 2, show the recorded ion mobility spectra of CAF with corona discharge and UV ionization sources, respectively.

Table 4

The internal proton affinities, defined in R2 for the three most stable isomers of protonated caffeine at 473 K (in kcal/mol) using different levels of theory.

Reference compound	B3LYP/6-311++G**	CAM-B3LYP/6-311++G**	wB97X/6-311++G**
MH ⁺ (N8)	0	0	0
MH ⁺ (O11)	−5.667	−6.223	−6.612
MH ⁺ (O12)	−6.641	−6.821	−6.915

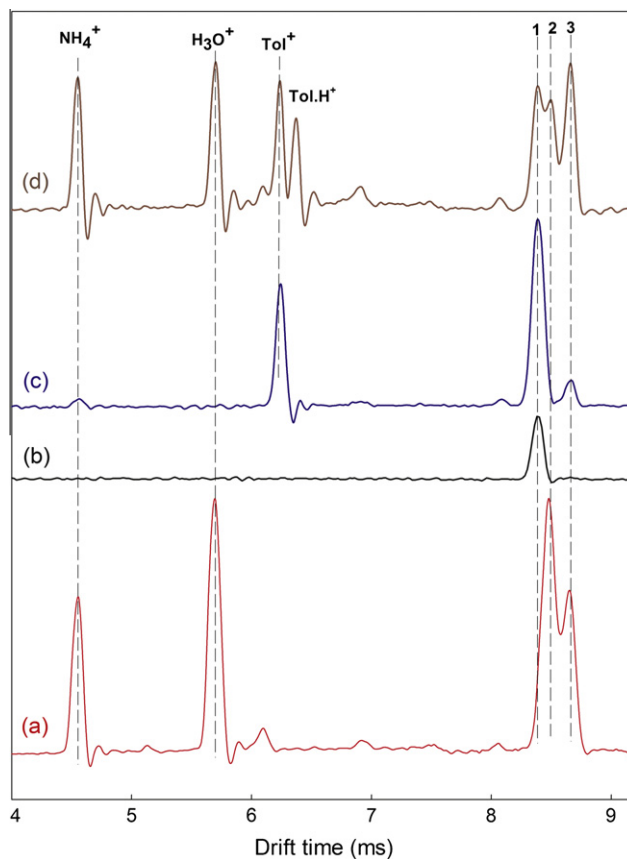
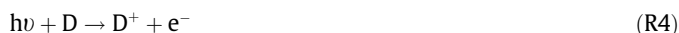


Fig. 2. Ion mobility spectra of caffeine recorded with; (a) corona discharge, (b) UV ionization, (c) dopant enhanced UV ionization and (d) simultaneous operation of the two sources with dopant. The ringing effect causes the response to drop below the baseline in the case of sharp peaks.

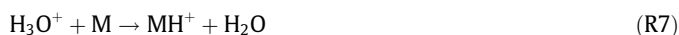
In the case of UV photoionization, dopant was added to enhance the ionization efficiency (trace *c*). As it is evident, the patterns of the spectra are different, depending on the kind of ionization source. The spectrum, which was recorded using CD, has two distinct peaks for CAF in the region of 8–9 ms, while the spectrum using UV source shows only one small peak in the corresponding region. In addition, in the presence of dopant, two separate peaks are observed in the UV ion mobility spectrum of CAF. The position of the peaks in the UV and CD spectra slightly differs. To ensure that the slight difference in position is not due to experimental error, the spectrum was recorded with simultaneous running of the two sources, trace *d*. Comparison of the trace *d* with that of *a* and *b* shows that the peak 1 is absent in CD spectrum and peak 2 is absent in UV spectrum. Hence, peak 1 originates from the UV and peak 2 comes from the CD ionization source. In addition, a new peak in trace *d* appears at about 6.4 ms, which is absent in other traces. This peak corresponds to the protonated toluene (Tol.H⁺) which is due to the presence of toluene in CD described in Ref. 36

3.4. Peaks assignment

The exact assignment of the peaks in ion mobility spectra needs a mass spectrometer coupled to the IMS. However, based on some evidence and experimental observation, some speculations may be given. The ionization energy of CAF (7.95 or 8.50 eV [40]) is lower than the UV photon energy (10 and 10.6 eV). Hence, CAF is expected to be directly photoionized by the UV source. The UV spectrum shows only one peak, which can be attributed to the M^+ ions (peak 1). By adding toluene as dopant to the ionization source, the tol^+ peak appears (trace c). In addition, the intensity of the M^+ peak is increased and a second peak appears. In the presence of dopant, the M^+ ion originates through indirect ionization via charge transfer between dopant photoion and CAF. The new small peak could be assigned to MH^+ formed via proton abstraction from the dopant photoion, which is less probable than the charge transfer [41]. The whole mechanism may be written as;



In the case of CD ionization, the major mechanism is proton transfer reaction from the reactant ion, $(H_2O)_nH^+$, to the analyte.



Based on the UV observations, the peak 3 in CD spectrum is assigned to MH^+ . However, the assignment of the peak 2 is a challenge. One may refer to a fragment ion due to dissociation of protonated CAF. However, mass spectrometry studies show that CAF do not dissociate in CD ionization [7]. In addition, if the peak 2 originated from a CAF fragment, it would appear before the M^+ peak, which is not true.

IMS-Mass studies of CAF show the only the m/z 195 as the major ion [14]. Hence, the peaks 2 may be assigned to different forms of protonated CAF other than that corresponding to peak 3. This assumption is supported by theoretical calculations presented in Section 3.1, which gives three stable forms for protonated CAF.



The question now is which peak belongs to what stable isomer. This is discussed in detail in the next sections based on some additional experiments.

3.4.1. The effect of concentration

The relative intensity of peaks 2 and 3 depends on the amount of CAF injected to the IMS ionization region. Fig. 3 shows the ion mobility spectra of caffeine at three different concentrations with CD as the ionization source. At low concentrations, the peak 2 is more intense than the peak 3, but the relative intensities are swapped at high concentrations. At very high concentration of CAF, the peak 2 disappeared (not shown).

The change in the relative intensities with concentration can be explained by the concept of IPA, described earlier. The analyte itself can play the role of the third body in Reaction 3. i.e.



Increasing the concentration of M pushes forward the reaction to the most stable isomer ion. Table 2 shows that the most stable form of $CAF.H^+$ is the $MH^+(N8)$. Peak 3 is attributed to the most sta-

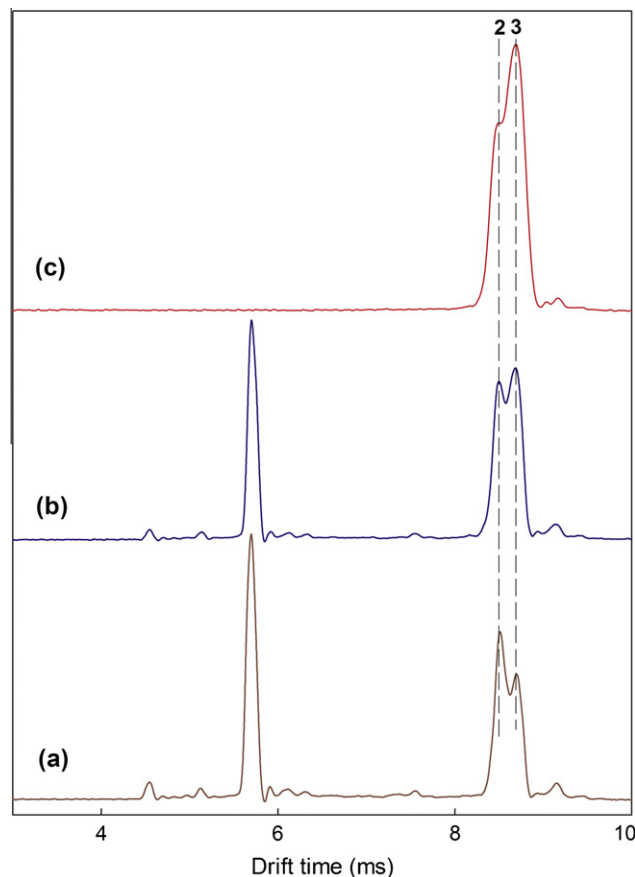


Fig. 3. Ion mobility spectrum of caffeine with CD ionization source for three different concentrations; (a) 5 ppm, (b) 20 ppm and (c) 70 ppm.

ble isomer, $MH^+(N8)$, since at high concentration, thermodynamics is governing the reaction and only peak 3 exists.

At low concentrations, the proton transfer reaction from the reactant ion to the analyte is kinetic control and the ratio of the products in parallel reactions of (R6–8) is mainly governed by the probability for protonation of the sites. Hence, all three forms of MH^+ are produced. The two forms of $MH^+(O11$ and $O12)$ are similar in terms of energy and structure. They are expected to appear at the same drift time, boosting the total intensity higher than that of the $MH^+(N8)$. As a conclusion, the peak 2 and 3 are assigned to $MH^+(O)$ and $MH^+(N8)$, respectively.

3.4.2. Ammonium reactant ion

Addition of ammonia to the ionization source lowers the proton transfer ionization efficiency of less-basic compounds. Due to the high PA, ammonia reacts with hydronium ions to form ammonium reactant ions,



The effect of the addition of ammonia on CAF spectrum is shown in Fig. 4.

In ion mobility spectra of CAF with H_3O^+ reactant ion, the peak 2 is bigger than the peak 3, while introducing ammonia annihilates the H_3O^+ peak and swaps the order of intensities for the peaks 2 and 3. The change in intensities is probably due to the fact that the N8 site, rather than the O11 or O12 site, more favors taking the proton from NH_4^+ . In other words, the IPA of the N8 protonated isomer is higher than that of the carbonyl oxygens. It is noteworthy that although the relative intensity of the peaks was changed, none of the CAF peaks was eliminated. This is because of higher

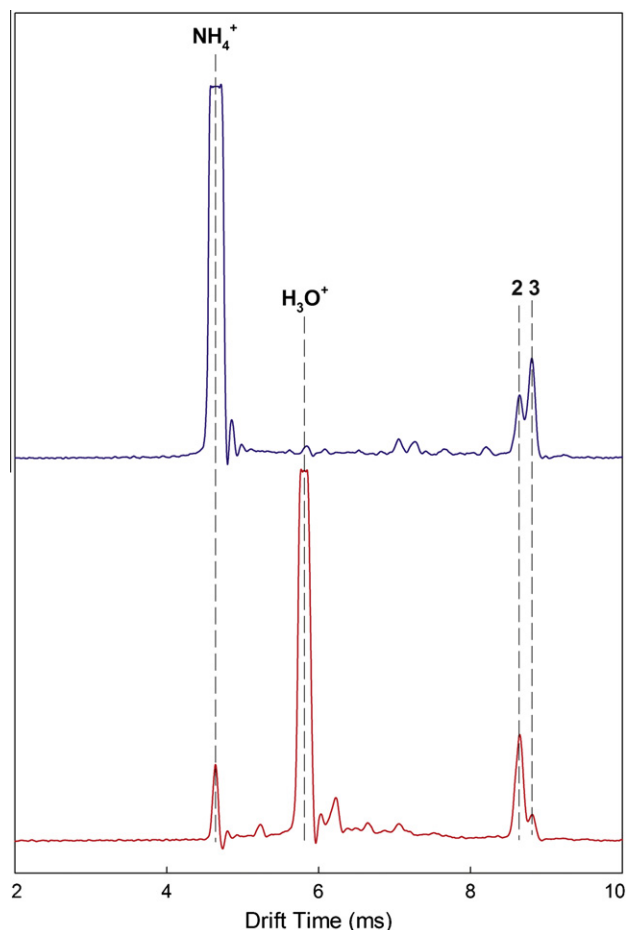


Fig. 4. Ion mobility spectrum of caffeine using CD ionization source with hydroxium reactant ion (bottom) in comparison with ammonium reactant ions (above).

proton affinity of CAF in all three forms, as compared with that of ammonia. Calculated proton affinities, presented in Table 3, support this assumption.

3.5. The peak positions

As shown in Fig. 2, the three peaks observed for CAF are denoted by 1, 2 and 3 in the ion mobility spectrum with two ionization sources. Peak 1 was attributed to the M^+ ion while peak 2 and 3, with higher drift times, were assigned to $MH^+(O)$ and $MH^+(N8)$, respectively. One may question the separation of these very similar ions in IMS, mainly because of low resolution of the technique. It should be mentioned that the separation of isomers has often been observed in IMS [32,33]. Unlike mass spectrometry, separation of

ions in IMS depends not only on mass, but also on size and shape. Revercomb and Mason [42] have derived the general theory for the mobility of ions as;

$$K = \frac{3}{16} \frac{q}{N} \left(\frac{1}{m} + \frac{1}{M} \right)^{1/2} \left(\frac{2\pi}{kT} \right)^{1/2} \frac{1}{\Omega_D} \quad (E1)$$

where K is ion mobility, q is the ion charge, N is the number density of the drift gas, m and M are the masses of the ion and the buffer gas, k is the Boltzmann constant, T is the temperature in Kelvin, and Ω_D is the ion–neutral collision cross section. The ion's structural features are represented by collision cross section. In fact, the term Ω_D provides information about the three dimensional structures of ions and electronic factors related to the ion–neutral interaction forces [43]. We used the calculated volume and surface area as a shape indicator and dipole moment of caffeine related ions as well as the charge distribution as an indicator for electronic factor to exhibit a rational explanation for CAF peaks separation in IMS. All calculations were performed at two levels of theory, HF/aug-cc-pVDZ and B3LYP/6-311++G**.

3.5.1. Volume and surface area calculations

The three-dimensional structure of ion has an important role in the collision cross section and therefore, in ion mobility, which determines the drift time. To obtain an indicator for the size, molecular volume of neutral caffeine and its related ions were calculated using the keyword “Volume” in Gaussian software. Estimating the molecular volumes is based on the numerical Monte Carlo integration, which has a large degree of error, to reduce the random error, the keyword SCF = Tight Volume = Tight (as in Parsons and Ninham [44]) was used and the volume calculations were repeated 10 times for each species. The *ab initio* average volumes for CAF and its related ions are along with standard deviation tabulated in Table 5.

As another shape indicator, we use the cavity volume and surface area from PCM (Polarizable Continuum Model) for comparison of the shapes [45]. PCM is one of the most frequently used continuum solvation methods for calculating molecular free energy in solution. The calculation, initiated by defining a cavity through interlocking van der Waals-spheres, is centered at atomic positions.

As shown in Table 5, The N8 protonated isomer shows a greater volume and surface area than oxygen protonated isomers. On the other hand, the M^+ ion has the lowest Volume. However, the difference in volume is not considerable and in the case of gas phase, it is less than the standard deviation; hence the volume, by itself, is not the dominant factor to govern the peak positions. Other factors such as dipole moment and charge distribution may be more influenced by the drift times.

3.5.2. Charge distribution and dipole moments

Neutral molecules including the buffer gas molecule and trace amount of water molecules are polarized by the field created by

Table 5
The calculated average volumes of most stable structures of caffeine and its related ions at HF/aug-cc-pVDZ and B3LYP/6-311++G** level of theory in gas phase as well as PCM model.

Compound	HF/aug-cc-pvdz			B3LYP/6-311++G**		
	V_a (cm ³ /mol)	V (Å ³) ^[a]	SA (Å ²) ^[a]	V_a (cm ³ /mol)	V (Å ³)	SA (Å ²)
Caffeine (M)	135.1 ± 6.3	194.217	216.824	138.6 ± 5.3	195.705	218.369
M+	127.5 ± 5.5	194.797	217.379	131.3 ± 3.6	196.096	218.855
M(N8)-H+	128.2 ± 5.5	196.743	219.361	133.4 ± 5.7	198.227	220.934
M(O11)-H+	127.7 ± 5.6	195.902	218.007	132.7 ± 5.4	197.537	219.789
M(O12)-H+	129.9 ± 5.3	196.437	218.450	136.1 ± 4.6	198.119	220.260

^[a]Calculated by PCM model.

Table 6

Dipole moments (in Debye) for caffeine and its related ions as well as the local charge on the added proton for protonated caffeine isomers.

Compound	B3LYP/6-311++G**		wB97X/6-311++G**	
	Dipole moment	Proton Charge	Dipole moment	Proton Charge
Caffeine (M)	4.0180	-	4.0539	-
M ⁺	4.4916	-	4.6681	-
M(N8)-H ⁺	9.7276	0.3888	10.0456	0.4097
M(O11)-H ⁺	5.4189	0.3281	5.6353	0.3352
M(O12)-H ⁺	2.8028	0.3526	3.0385	0.3584

the dipole moment and the charge of the ion. Greater dipole moment results in stronger ion–neutral interaction, which leads to less mobility and longer drift time. In addition, localizing the ion charge on a specific atom creates a strong field which attracts the neutral molecules. If the charge is focused on the added proton, it attracts water molecules to form hydrated ion via hydrogen bonding. This leads to a considerable change in the size and as a consequence, the drift time. Table 6 shows the dipole moment of CAF and its related ions at two levels of theory.

The results show that the N8 protonated isomer has a significantly higher dipole moment when compared with those of oxygen protonated isomers. This observation indicates that MH⁺(N8) isomer has more interaction with neutral gasses in the drift tube and therefore, higher drift time. In addition, the charge density on the proton in the N8 isomer is higher than that in other isomers. This leads to higher hydration tendency, which causes a longer drift time. It should be mentioned that based on calculation, the M⁺ ion is not hydrated while all protonated forms show a considerable tendency for hydration. This is the reason for separation of M⁺ ion from MH⁺ ion, despite a minor difference in mass and volume.

4. Conclusions

The experimental and theoretical results show that caffeine is ionized to M⁺ with the UV ionization source, while it is protonated in the corona discharge without fragmentation. In spite of no fragmentation, the corona discharge ion mobility spectrum of caffeine has two distinct peaks. The peaks, which are well separated, were attributed to different protonated isomers. The separation of isomers is mostly due to the difference in their interaction with buffer gas and trace water molecules. Calculation showed that the most stable protonated isomer is the one in which proton is attached to the (imine nitrogen) N8 atom. Through the study of concentration effect and the role of reactant ion in the relative intensities, the most stable isomer was identified to be the one with the longest drift time. This assumption was confirmed with further calculations on volume, charge density and dipole moment. The N8 protonated isomer has the largest dipole moment and bigger volume and more localized charge on the added proton, all together resulting in strong interaction with buffer gas, which, in turn, leads to the longest drift time with respect to other isomers.

Finally, the concept of “internal proton affinity” (IPA) which reflects the internal competition for proton exchange among the different atoms in multifunctional molecules, was introduced. Like proton affinity values, the new quantity helps to find out the possible protonated forms of a given molecule other than the most stable one. In IMS, if the Δ PA is larger than the IPA, where Δ PA is the difference in proton affinities between the analyte and water (or ammonia), the corresponding protonated isomer has the chance to be formed in the ionization region.

Acknowledgements

The authors would like to acknowledge the financial support of the Center of Excellence for Sensor and Green Chemistry. Also, the authors would like to appreciate F. Fathi and V. Ilbeigy for their invaluable assistance.

References

- [1] A. Nehlig, J.L. Daval, G. Debry, *Brain Res. Rev.* 17 (1992) 139.
- [2] M. Thevis, G. Opfermann, O. Krug, W. Schänzer, *Rapid Commun. Mass Spectrom.* 18 (2004) 1553.
- [3] M. Aranda, G. Morlock, *Rapid Commun. Mass Spectrom.* 21 (2007) 1297.
- [4] S. Zhou, K.D. Cook, *J. Am. Soc. Mass Spectrom.* 11 (2000) 961.
- [5] D.B. Robb, T.R. Covey, A.P. Bruins, *Anal. Chem.* 72 (2000) 3653.
- [6] D.I. Carroll, I. Dzidic, R.N. Stillwell, M.G. Horning, E.C. Horning, *Anal. Chem.* 46 (1974) 706.
- [7] I.M. Lazar, M.L. Lee, *Anal. Chem.* 68 (1996) 1924.
- [8] Y. Zhang, N. Mehrotra, N.R. Budha, M.L. Christensen, B. Meibohm, *Clin. Chim. Acta* 398 (2008) 105.
- [9] M. Pellegrini, E. Marchei, S. Rossi, F. Vagnarelli, A. Durgbanshi, O. Garcia-Algar, O. Vall, S. Pichini, *Rapid Commun. Mass Spectrom.* 21 (2007) 2693.
- [10] J.D. Dunn, C.M. Gryniewicz-Ruzicka, J.F. Kauffman, B.J. Westenberg, L.F. Buhse, *J. Pharm. Biomed. Anal.* 54 (2011) 469.
- [11] F. Malekahmadi, M.Sc. thesis, Isfahan University of Technology (IR), 2011.
- [12] N. Budimir, D.J. Weston, C.S. Creaser, *Analyst* 132 (2007) 34.
- [13] R. Fernández-Maestre, H.H. Hill Jr., *Int. J. Ion Mobil. Spec.* 12 (2009) 91.
- [14] M.J. Waltman, P. Dwivedi, H.H. Hill Jr, W.C. Blanchard, R.G. Ewing, *Talanta* 77 (2008) 249.
- [15] G.A. Eiceman, D.A. Blyth, D.B. Shoff, A.P. Snyder, *Anal. Chem.* 62 (1990) 1374.
- [16] J.E. Szulejko, T.B. McMahon, *Int. J. Mass Spectrom. Ion Processes* 109 (1991) 279.
- [17] J.E. Szulejko, T.B. McMahon, *J. Am. Chem. Soc.* 115 (1993) 7839.
- [18] K.B. Green-Church, P.A. Limbach, *J. Am. Soc. Mass Spectrom.* 11 (2000) 24.
- [19] F. Greco, A. Liguori, G. Sindona, N. Uccella, *J. Am. Chem. Soc.* 111 (1990) 9092.
- [20] M. Decouzou, J.F. Gal, M. Herreros, P.C. Maria, J. Murrell, J.F.J. Todd, *Rapid Commun. Mass Spectrom.* 10 (1996) 242.
- [21] S.A.H. Petrie, C.G. Freeman, M.J. McEwan, M. Meot-Ner (Mautner), *Int. J. Mass Spectrom. Ion Processes* 90 (1989) 241.
- [22] A.B. Raksit, D.K. Bohme, *Int. J. Mass Spectrom. Ion Processes* 57 (1984) 211.
- [23] M. Tabrizchi, S. Shoostari, *J. Chem. Thermodyn.* 35 (2003) 863.
- [24] F. Pepi, A. Ricci, M.D. Stefano, M. Rosi, *Phys. Chem. Phys.* 7 (2005) 1181.
- [25] K. Zhang, D.M. Zimmerman, A.C. bung-Phillips, C.J. Cassidy, *J. Am. Chem. Soc.* 115 (1993) 10812.
- [26] C.J. Cassidy, S.R. Cam, K. Zhang, A. Chung-Phillips, *J. Org. Chem.* 60 (1995) 1704.
- [27] A. Akrou, Z. Chikh, F. Djazi, M. Elbannay, F. Berruyer, G. Bouchoux, *Int. J. Mass Spectrom.* 267 (2007) 63.
- [28] M. Rožman, *Chem. Phys. Lett.* 543 (2012) 50.
- [29] Z.B. Maksić, B. Kovačević, A. Lesar, *Chem. Phys.* 253 (2000) 59.
- [30] J. Smets, L. Houben, K. Schoone, G. Maes, L. Adamowicz, *Chem. Phys. Lett.* 262 (1996) 789.
- [31] J.K. Wolken, F. Turecek, *J. Am. Soc. Mass Spectrom.* 11 (2000) 1065.
- [32] H. Borsdorf, E.G. Nazarov, G.A. Eiceman, *J. Am. Soc. Mass Spectrom.* 13 (2002) 1078.
- [33] H. Borsdorf, M. Rudolph, *Int. J. Mass Spec.* 208 (2001) 67.
- [34] M. Tabrizchi, “Research Grade Ion Mobility Spectrometer”, Iranian Patent, 42767, 2005.
- [35] M. Tabrizchi, H. Bahrami, *Anal. Chem.* 83 (2011) 9017.
- [36] H. Bahrami, M. Tabrizchi, *Talanta* 97 (2012) 400.
- [37] M.J. Frisch, G.W. Trucks, H.B. Schlegel, G.E. Scuseria, M.A. Robb, J.R. Cheeseman, G. Scalmani, V. Barone, B. Mennucci, G.A. Petersson, H. Nakatsuji, M. Caricato, X. Li, H.P. Hratchian, A.F. Izmaylov, J. Bloino, G. Zheng, J.L. Sonnenberg, M. Hada, M. Ehara, K. Toyota, R. Fukuda, J. Hasegawa, M. Ishida, T. Nakajima, Y. Honda, O. Kitao, H. Nakai, T. Vreven, J.A. Montgomery, Jr., J.E. Peralta, F. Ogliaro, M. Bearpark, J.J. Heyd, E. Brothers, K.N. Kudin, V.N. Staroverov, T. Keith, R. Kobayashi, J. Normand, K. Raghavachari, A. Rendell, J.C. Burant, S.S. Iyengar, J. Tomasi, M. Cossi, N. Rega, J.M. Millam, M. Klene, J.E. Knox, J.B. Cross, V. Bakken, C. Adamo, J. Jaramillo, R. Gomperts, R.E. Stratmann, O. Yazyev, A.J. Austin, R. Cammi, C. Pomelli, J.W. Ochterski, R.L. Martin, K. Morokuma, V.G. Zakrzewski, G.A. Voth, P. Salvador, J.J. Dannenberg, S. Dapprich, A.D. Daniels, O. Farkas, J.B. Foresman, J.V. Ortiz, J. Cioslowski, D.J. Fox, *Gaussian 09, Revision B.01*, Gaussian, Inc., Wallingford CT, 2010.
- [38] J.E. Bartmess, *J. Phys. Chem.* 98 (1994) 6420.
- [39] C.S. Tautermann, A.F. Voegele, T. Loerting, K.R. Liedl, *J. Chem. Phys.* 117 (2002) 1962.
- [40] <http://webbook.nist.gov>.
- [41] D.B. Robb, M.W. Blades, *Anal. Chim. Acta* 627 (2008) 34.
- [42] H.E. Revercomb, E.A. Mason, *Anal. Chem.* 47 (1975) 970.
- [43] S.N. Lin, G.W. Griffin, E.C. Horning, W.E. Wentworth, *Chem. Phys.* 60 (1974) 4994.
- [44] D.F. Parsons, B.W. Ninham, *J. Phys. Chem. A* 113 (2009) 1141.
- [45] S. Miertus, E. Scrocco, J. Tomasi, *Chem. Phys.* 55 (1981) 117.